CHEMISTRY & SUSTAINABILITY
CHEMSUSCHEM
ENERGY & MATERIALS

Supporting Information

Solar-Driven H_2O_2 Generation From H_2O and O_2 Using Earth-Abundant Mixed-Metal Oxide@Carbon Nitride Photocatalysts

Ruirui Wang,[a] Kecheng Pan,[a] Dandan Han,[a] Jingjing Jiang,[b] Chengxiang Xiang,[b] Zhuangqun Huang,[b, c] Lu Zhang,[a, b] and Xu Xiang*[a]

cssc_201600705_sm_miscellaneous_information.pdf

Solar-Driven Hydrogen Peroxide Generation Only From Water and Oxygen Using Earth-Abundant Mixed-Metal Oxide@Carbon Nitride Composite Photocatalysts

Ruirui Wang [a], Kecheng Pan [a],Dandan Han [a], Jingjing Jiang[b],Chengxiang Xiang [b], Zhuangqun Huang [b,c], Lu Zhang [a, b], Xu Xiang [a]*

[a]State Key Laboratory of Chemical Resource Engineering,
Beijing University of Chemical Technology, Beijing 100029 PR China
[b] Joint Center for Artificial Photosynthesis, California Institute of Technology,
Pasadena, California, 91125USA
[c] AFM Business Unit, Bruker Nano Surfaces, Santa Barbara, California, 93117USA

[*] Email: xiangxu@mail.buct.edu.cn

Figure captions

Figure S1 AFM images of (A) C_3N_4, (B) MMO@C_3N_4, (C) C_3N_4, and (D) MMO@C_3N_4 with different scales.

Figure S2 XRD pattern of the monometallic nickel sample calcined at 300 ^oC.

Figure S3 XRD pattern of the monometallic ferric sample calcined at 300 ^oC.

Figure S4 FTIR spectra of MMO@C_3N_4 and C_3N_4.

Figure S5 The H_2O_2 generation in O_2-equilibrated condition over MMO@C_3N_4 with and without light irradiation. 1 gL^{-1} photocatalyst, pH= 3, illumination intensity100 $mWcm^{-2}$.

Figure S6 The light-driven H_2O_2 generation in O_2- or N_2-saturated conditions, respectively. The experimental conditions were as follows: 1 gL^{-1}photocatalyst, pH=3, illumination intensity100 $mWcm^{-2}$.

Figure S7 The effect of MMO content in the MMO@C_3N_4 on the photocatalytic H_2O_2 production.1 g L^{-1} photocatalyst, pH= 3, illumination intensity 100 mW cm^{-2}.

Figure S8 Kinetic curves of (A) MMO@C_3N_4, (B) MMO/C_3N_4 -Mix, (C) Ni@C_3N_4 and (D) Fe@C_3N_4.

Figure S9 The light-driven H_2O_2 generation in O_2-equilibrated conditions over MMO@C_3N_4: recycled use of catalyst up to 5 times. 1 gL^{-1} photocatalyst, pH= 3, illumination intensity 100 $mWcm^{-2}$.

Figure S10 FTIR spectra of MMO@C_3N_4 before and after catalytic reactions.

Figure S11 XRD patterns of MMO@C_3N_4 before and after catalytic reactions.

Figure S12 HRTEM images of MMO@C_3N_4 after catalytic reactions.

Figure S13 Fitting of H_2O_2 decomposition, following first-order kinetics model.

Figure S14 The pH effect on H_2O_2 generation in O_2-equilibrated conditions over MMO@C_3N_4. 1 g L^{-1} photocatalyst, illumination intensity 100 mW cm^{-2}.

FigureS15 The H_2O_2 generation in O_2-equilibrated condition over C_3N_4(urea). 1 g L^{-1} photocatalyst, pH= 3, illumination intensity 100 mW cm^{-2}.

FigureS16 Linear sweep voltammetry (LSV) curves of catalyst-loaded electrodes for LDH@C_3N_4 and MMO@C_3N_4 toward OER in acidic solution (pH 3), scan rate 10 mV s^{-1}.

Figure S17 The H_2O_2 generation in O_2-equilibrated condition over MMO@C_3N_4 and LDH@C_3N_4. 1 g L^{-1} photocatalyst, pH= 3, illumination intensity 100 mW cm^{-2}.

Figure S18 Tauc plots of C_3N_4 and MMO@C_3N_4.

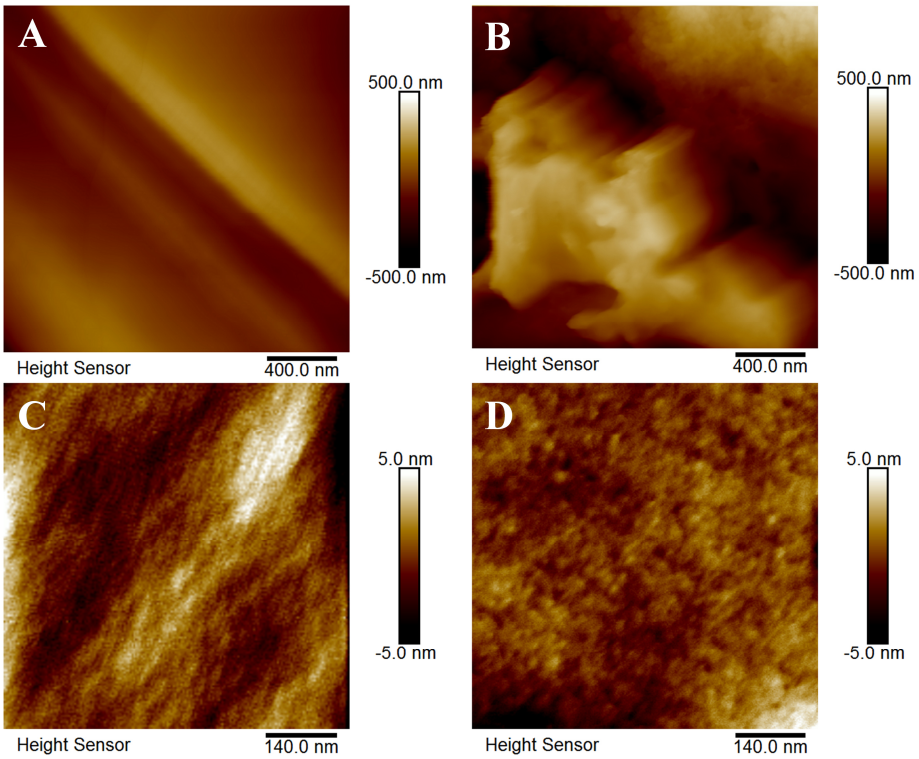

Figure S1 AFM images of (A) C_3N_4, (B) MMO@C_3N_4, (C) C_3N_4, and (D) MMO@C_3N_4 with different scales.

In **Figure S2 and S3**, the XRD patterns were indexed to $Ni(HCO_3)_2$ (JCPDS 15-0782) and hematite (α-Fe_2O_3, JCPDS 33-0664) phase for the nickel and ferric samples, respectively.

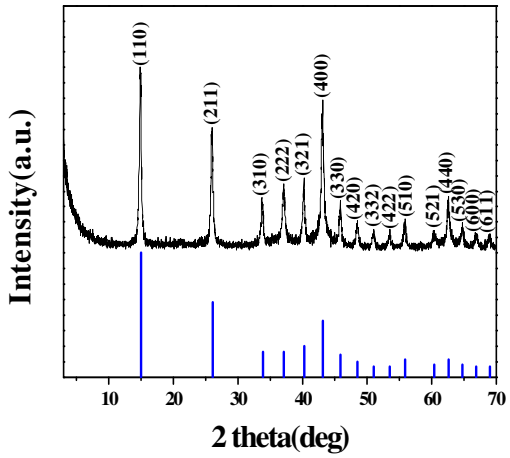

Figure S2 XRD pattern of the monometallic nickel sample calcined at 300 ^{o}C.

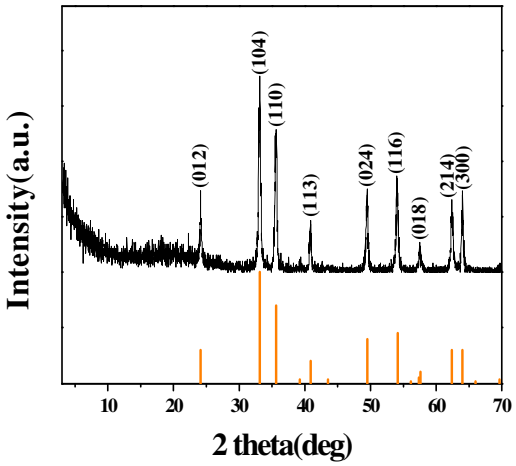

Figure S3 XRD pattern of the monometallic ferric sample calcined at 300 ^{o}C.

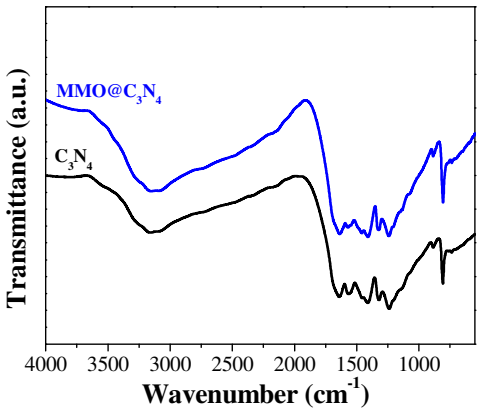

Figure S4 FTIR spectra of MMO@C_3N_4 and C_3N_4

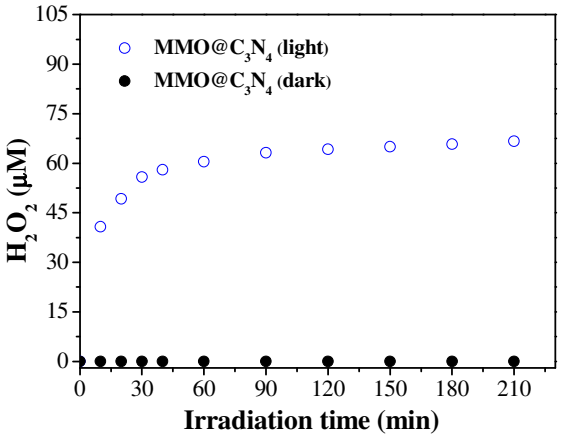

Figure S5 The H_2O_2 generation in O_2-equilibrated condition over MMO@C_3N_4 with and without light irradiation. The experimental conditions were as follows: 1 gL^{-1} photocatalyst, pH= 3, illumination intensity100 $mWcm^{-2}$.

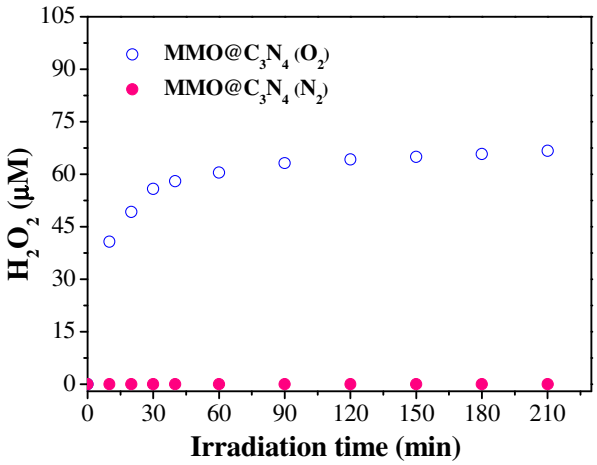

Figure S6 The light-driven H_2O_2 generation in O_2- or N_2-saturated conditions, respectively. The experimental conditions were as follows: 1 gL^{-1} photocatalyst, pH=3, illumination intensity100 mW cm^{-2}.

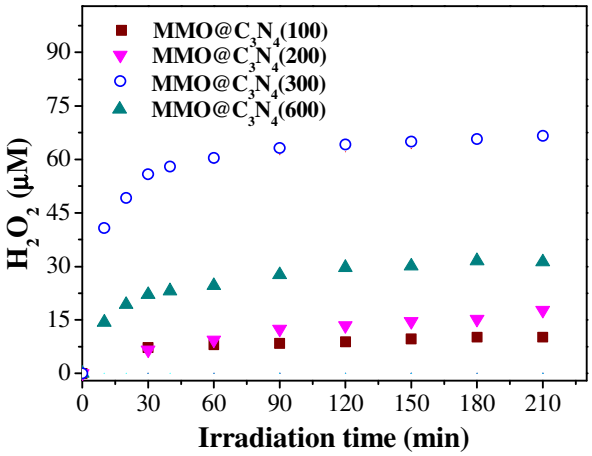

Figure S7 The effect of MMO content in the MMO@C_3N_4 on the photocatalytic H_2O_2 production. 1 g L^{-1} photocatalyst, pH= 3, illumination intensity 100 mW cm^{-2}.

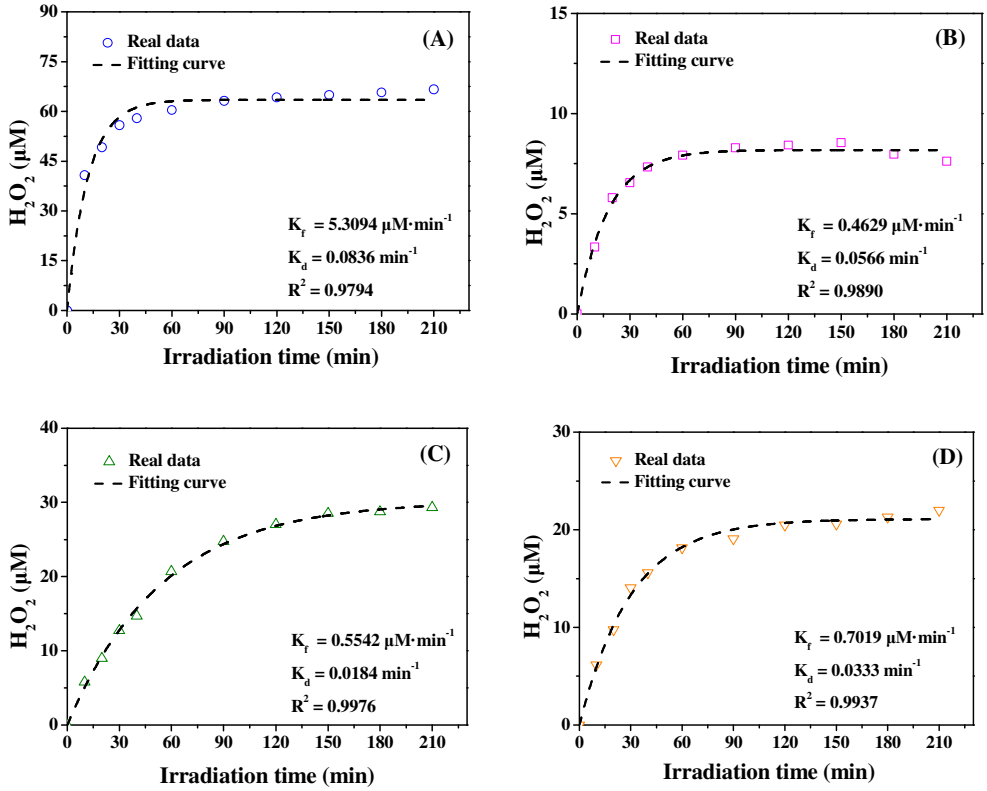

Figure S8 Kinetic curves of (A) MMO@C_3N_4, (B) MMO/C_3N_4 -Mix, (C) Ni@C_3N_4 and (D) Fe@C_3N_4.

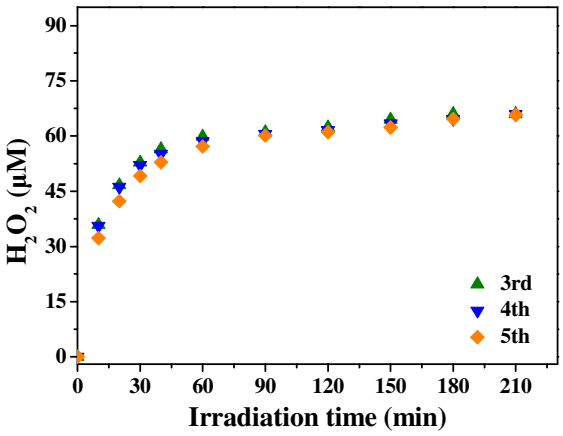

Figure S9 The light-driven H_2O_2 generation in O_2-equilibrated conditions over MMO@C_3N_4: recycled use of catalyst up to 5 times. 1 gL^{-1} photocatalyst, pH= 3, illumination intensity 100 mW cm^{-2}.

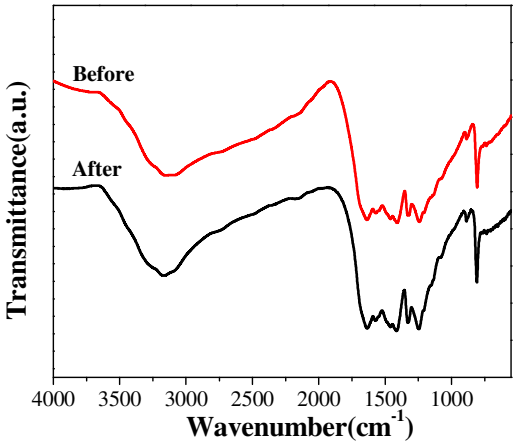

Figure S10 FTIR spectra of MMO@C_3N_4 before and after catalytic reactions.

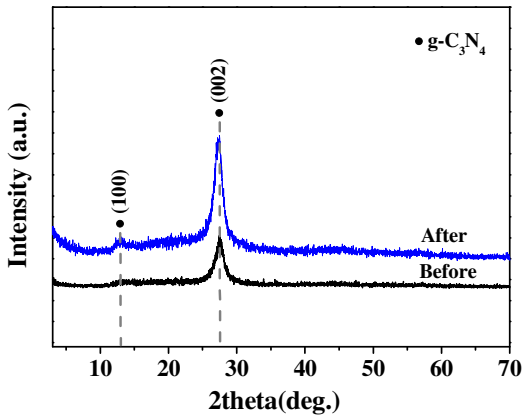

Figure S11 XRD patterns of MMO@C_3N_4 before and after catalytic reactions.

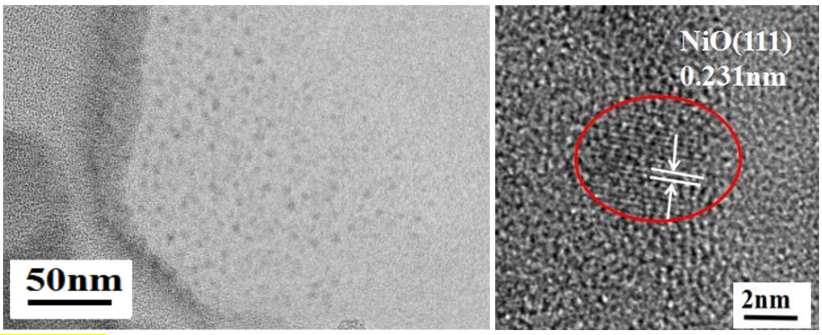

Figure S12 HRTEM images of MMO@C_3N_4 after catalytic reactions.

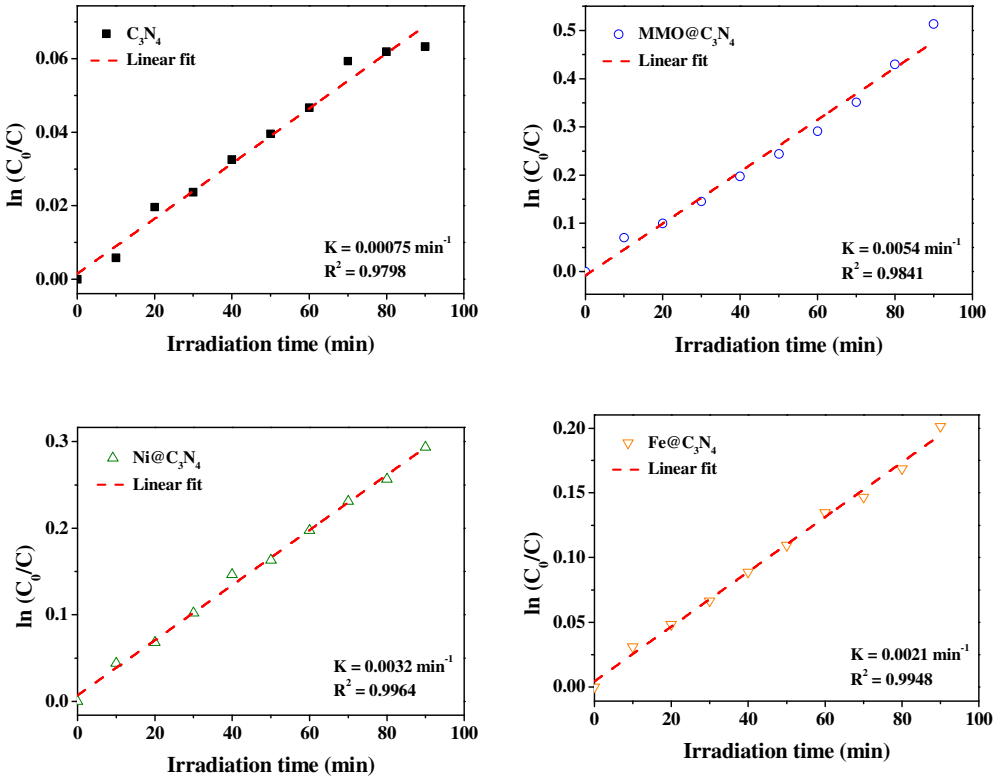

Figure S13 Fitting of H_2O_2 decomposition, following first-order kinetics model.

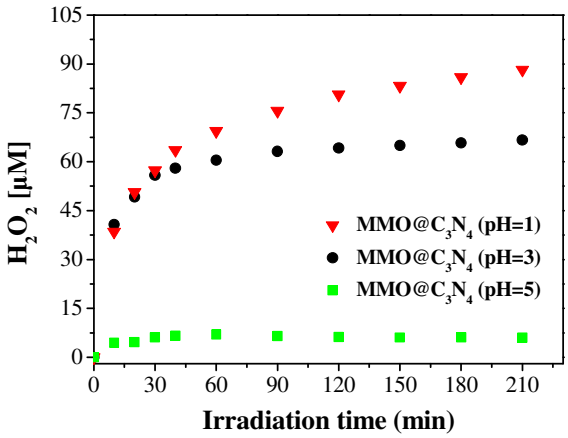

Figure S14 The pH effect on H_2O_2 generation in O_2-equilibrated conditions over MMO@C_3N_4. 1 g L^{-1} photocatalyst, illumination intensity 100 $mWcm^{-2}$.

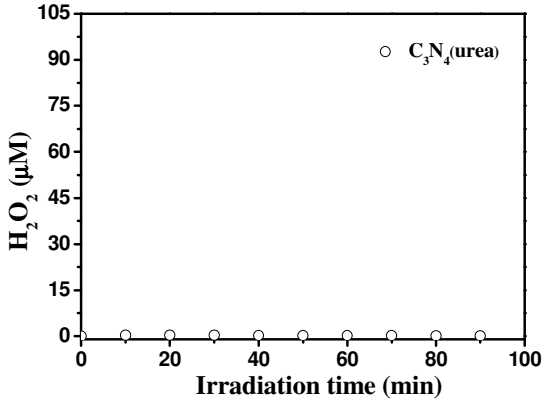

Figure S15 The H_2O_2 generation in O_2-equilibrated condition over C_3N_4(urea).

1 g L^{-1} photocatalyst, pH= 3, illumination intensity 100 mW cm^{-2}.

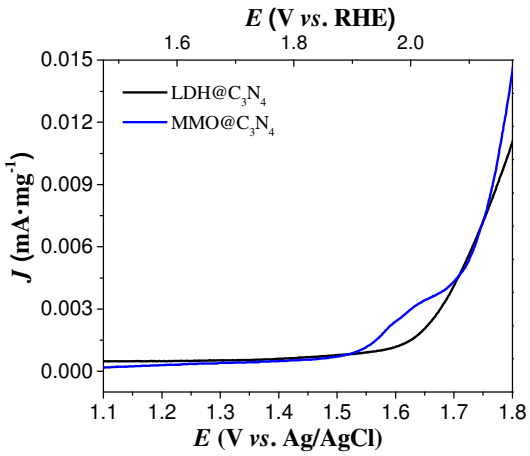

Figure S16 Linear sweep voltammetry (LSV) curves of catalyst-loaded electrodes for $LDH@C_3N_4$ and $MMO@C_3N_4$ toward OER in acidic solution (pH 3), scan rate 10 mV s^{-1}.

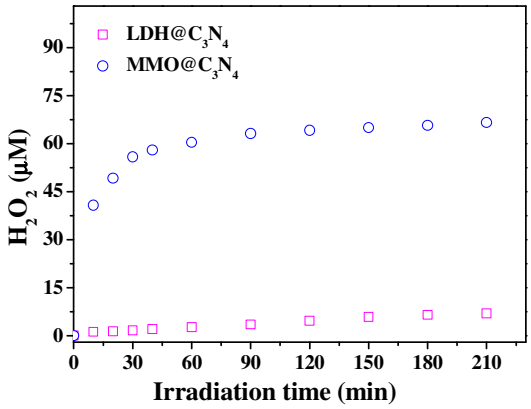

Figure S17 The H_2O_2 generation in O_2-equilibrated condition over MMO@C_3N_4 and LDH@C_3N_4. 1 g L^{-1} photocatalyst, pH= 3, illumination intensity 100 mW cm^{-2}.

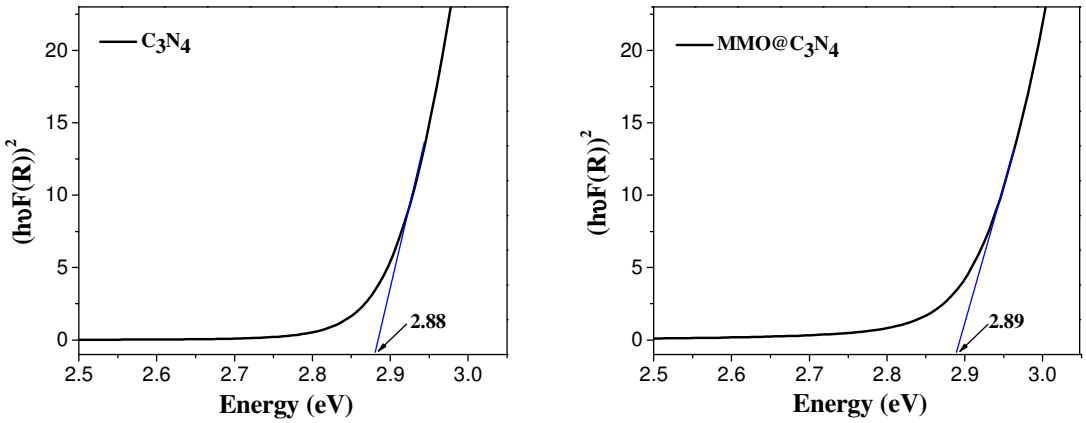

Figure S18 Tauc plots of C_3N_4 and MMO@C_3N_4.